applied sciences

MDPI

Article

Ca-Alginate-PEGMA Hydrogels for In Situ Delivery of TGF-β Neutralizing Antibodies in a Mouse Model of Wound Healing

Jahaziel Gasperin-Bulbarela [1], Ana B. Castro-Ceseña [1,2], Tanya Camacho-Villegas [3,4], Pavel H. Lugo-Fabres [3,4], Nestor Emmanuel Díaz-Martínez [3], Eduardo Padilla-Camberos [3], Raquel Echavarría [5] and Alexei F. Licea-Navarro [1,*]

1 Departamento de Innovación Biomédica, Centro de Investigación Científica y de Educación Superior de Ensenada (CICESE), Carretera Ensenada-Tijuana No. 3918, Zona Playitas, Ensenada C.P. 22860, Baja California, Mexico; jgasperi@cicese.edu.mx (J.G.-B.); abcastroca@conacyt.mx (A.B.C.-C.)
2 CONACYT-Centro de Nanociencias y Nanotecnología, Universidad Nacional Autónoma de México, Km 107 Carretera Tijuana-Ensenada, Ensenada C.P. 22860, Baja California, Mexico
3 Unidad de Biotecnología Médica y Farmacéutica, Centro de Investigación y Asistencia en Tecnología y Diseño del Estado de Jalisco (CIATEJ), A.C. Av. Normalistas 800 Colinas de la Normal, Guadalajara C.P. 44270, Jalisco, Mexico; tcamacho@ciatej.mx (T.C.-V.); plugo@ciatej.mx (P.H.L.-F.); ediaz@ciatej.mx (N.E.D.-M.); epadilla@ciatej.mx (E.P.-C.)
4 CONACYT-Unidad de Biotecnología Médica y Farmacéutica, Centro de Investigación y Asistencia en Tecnología y Diseño del Estado de Jalisco (CIATEJ), A.C. Av. Normalistas 800, Colinas de la Normal, Guadalajara C.P. 44270, Jalisco, Mexico
5 CONACyT-Centro de Investigación Biomédica de Occidente, Instituto Mexicano del Seguro Social, Guadalajara C.P. 44340, Jalisco, Mexico; rechavarria@conacyt.mx
* Correspondence: alicea@cicese.mx; Tel.: +52-646-175-05-00

check for updates

Citation: Gasperin-Bulbarela, J.; Castro-Ceseña, A.B; Camacho-Villegas, T.; Lugo-Fabres, P.H; Díaz-Martínez, N.E.; Padilla-Camberos, E.; Echavarría, R.; Licea-Navarro, A.F Ca-Alginate-PEGMA Hydrogels for In Situ Delivery of TGF-β Neutralizing Antibodies in a Mouse Model of Wound Healing. *Appl. Sci.* **2021**, *11*, 1164. https://doi.org/10.3390/app11031164

Received: 13 December 2020
Accepted: 22 January 2021
Published: 27 January 2021

Publisher's Note: MDPI stays neutral with regard to jurisdictional claims in published maps and institutional affiliations.

Copyright: © 2021 by the authors. Licensee MDPI, Basel, Switzerland. This article is an open access article distributed under the terms and conditions of the Creative Commons Attribution (CC BY) license (https://creativecommons.org/licenses/by/4.0/).

Abstract: Hydrogels provide effective alternatives for drug delivery when therapeutics cannot be applied directly to a wound, or if adverse effects are associated with systemic administration. However, drug delivery vehicles need to be biocompatible and biodegradable and exhibit sufficient mechanical strength to withstand handling and different physiological conditions, such as those encountered during topical administration of a therapeutic. Wound healing can be divided into three phases stimulated by transforming growth factor-beta (TGF-β) and, subsequently, targeted therapeutics have been developed to inhibit this cytokine for the treatment of chronic wounds and to prevent scarring. In this study, the capacity of calcium alginate hydrogels plasticized with poly(ethylene glycol) methyl ether methacrylate (PEGMA) to deliver anti-TGF-β antibodies (1D11.16.8) to a wound was investigated in situ. Three levels of antibodies, 10, 50, and 100 µg, were loaded into calcium-alginate-PEGMA hydrogels and evaluated in an excisional wound model in mice. Hydrogels containing 50 and 100 µg 1D11.16.8 produced less inflammation, accompanied by a marked reduction in collagen deposition and cell infiltration. These findings demonstrate the capacity of calcium-alginate-PEGMA hydrogels to deliver larger proteins, such as antibodies, to the site of a wound.

Keywords: hydrogel; wound healing; Ca-alginate; poly(ethylene glycol) methyl ether methacrylate; 1D11; TGF-β

1. Introduction

Wound healing is a dynamic process comprised of three overlapping phases, including inflammation, proliferation, and matrix remodeling, where any imbalance can lead to aberrant tissue formation known as fibrosis [1]. Transforming growth factor-beta (TGF-β) is a cytokine that exists in mammals as three different isoforms (TGF-β1, 2, and 3) and plays critical roles in wound healing and fibrosis [2]. Although the three isoforms activate the same receptor complex, they have slight differences in the signal transduction pathway. TGF-β1 participates throughout the wound healing process, promoting epithelial cell cycle

arrest, and with TGF-β2, recruiting fibroblast and immune cells and extracellular matrix (ECM) production [3,4], whereas TGF-β3 promotes epidermis migration and fetal scarless wounds [5,6]. The TGF-β signaling pathway is considered a promising target to improve wound healing outcomes in pathological wounds (such as hypertrophic scarring) or to prevent scarring in wounds produced by surgery or minor injuries [7]. Immunomodulatory treatments have been developed to target TGF-β signaling and prevent the action of this cytokine. Fresolimumab is one such treatment and a potent human monoclonal antibody that binds to and inhibits all isoforms of TGF-β. However, systemic administration of Fresolimumab is associated with adverse effects, such as keratoacanthomas, due to the complete neutralization of TGF-β [8,9]. To avoid adverse effects associated with systemic administration, therapies can be applied topically to elicit local effects. Hydrogels are one of the most attractive biomaterials for topical administration and are extremely useful when a therapy cannot be applied directly to a wound.

Polymeric matrices have been explored for the controlled release of proteins and other therapeutics, prolonging circulation half-life, and target-specific delivery [10,11]. One polymeric matrix is sodium alginate; a linear polysaccharide and copolymer derived from brown marine algae comprised of β-D-mannuronate (M) and α-L-guluronate (G) residues covalently linked in different alternating or random sequences, such as MMM, GGG, or MGM [12]. Alginate is used as a polymer in hydrogels because of its highly adsorptive capacity, high cost-effectiveness, biodegradability, and antibacterial characteristics [13]. Alginate hydrogels are also highly porous, contributing to the functionality of this matrix in wound dressings by keeping wounds moist without damaging newly formed tissue [14]. However, hydrogels based only on alginate exhibit poor structural stability that degrades further on contact with biological fluids due to loss of the crosslinker ion calcium (Ca^{2+}) [15]. To increase the handling and stability of alginate hydrogels, covalent or ionic crosslinking can be employed, or alginate can be combined with other biopolymers such as gelatin or chitosan [16–18]. Plasticizers are another excellent option to increase hydrogel stability because they reduce intermolecular forces between polymer chains, decrease brittleness, and increase flexibility, toughness, traction, and resistance; however, plasticizers also compromise the porosity of the resultant gel [19].

Recently, our group reported the impact of poly(ethylene glycol) methyl ether methacrylate (PEGMA) as a plasticizer in calcium alginate hydrogels. The addition of PEGMA created a spongious material composed of semispherical and interconnected 50–100 μm pores with increased stability in aqueous media and structural resistance to manipulation and bending [20]. To determine if Ca-alginate-PEGMA hydrogels (CAPH) could confer site-specific delivery of antibodies, a murine IgG1 pan-specific TGF-β neutralizing antibody, 1D11, was incorporated into CAPH [21]. The ID11 antibody was selected based on the capacity to neutralize the three isoforms of TGF-β and the implication of this cytokine in wound healing, and on previous studies reporting visible improvements in scarring, reduced infiltration of immune cells, less extracellular matrix (ECM) deposition of collagen fibers, and reduced vascularity observed following neutralization of TGF-β [22–24]. Therefore, the capacity of CAPH to release TGF-β neutralizing antibodies at the site of a wound and reduce the fibrotic effects of TGF-β was investigated in this study using a mouse model of dorsal bilateral excisional wound healing. Wound contraction ratio, collagen content, and wound healing assessment were determined to evaluate the activity of 1D11 and effectiveness of CAPH as a delivery vehicle.

2. Materials and Methods

2.1. Preparation of Composite Hydrogels

The CAPH solution was prepared as described elsewhere [20]. Briefly, 0.375% (*v*/*v*) PEGMA was homogenized with 1.5% (*w*/*v*) sodium alginate and cross-linked with 0.75% (*w*/*v*) calcium chloride with intensive stirring until a smooth solution was obtained. For hydrogel formation, CAPH solution was mixed with 1, 5, 10, 50, and 100 μg pan-specific anti-TGF-β mouse monoclonal antibody 1D11.16.8 (BioxCell, Lebanon, NH, USA) diluted

in Phosphate Buffered Saline (PBS), before being poured into a 96-well plate, frozen for 48 h at −20 °C, and lyophilized for another 24 h at −52 °C in a FreeZone 1-Liter Freeze dryer (Labconco, Kansas City, MO, USA). Empty hydrogels without antibody were also prepared and stored at 4 °C. In the remainder of this study, empty hydrogels are referred to as CAPH, while 1D11.16.8-loaded hydrogels are referred to as CAPH-1D11. For the in vitro assays described in Section 2.2, 0.1 μg of 1D11 antibody is enough to neutralize 20 pM of TGF-β (data are not shown), so hydrogels of 1 and 5 μg CAPH-1D11 were used, while 10, 50, and 100 μg CAPH-1D11 were explored in situ, as described in Section 2.3. The higher doses of 50 and 100 μg are to mimic the doses employed in previous works where neutralizing antibodies were injected [22,24,25].

2.2. HEK-Blue TGF-β SEAP Reporter Assay

The HEK-Blue TGF-β cell line (InvivoGen, San Diego, CA, USA) was used for in vitro assessment of TGF-β neutralization. Stimulation of these cells with TGF-β induces the Smad dependent pathway and secretion of secreted embryonic alkaline phosphatase (SEAP) into media that can be measured via QUANTI-Blue and spectrophotometry. Cells were maintained and assayed according to the manufacturer's protocol with modifications. Briefly, alginate hydrogels were incubated for 2 h in 1 mL Dulbecco's Modified Eagle Medium (DMEM) to release antibodies, then 2.5×10^4 cells (90 μL) were seeded into a 96-well plate before 20 pM (in 10 μL) recombinant human TGF-β1 (Peprotech, Cranbury, NJ, USA) was used to stimulate the cells. Next, 100 μL alginate hydrogels pre-conditioned media was added to the cells. Two activity controls included TGF-β treatment of cells with DMEM without hydrogels and cells incubated only with DMEM (without TGF-β). Cells were incubated for 24 h at 37 °C and 5% CO_2. Media (10 μL) were transferred to a new plate and mixed with 90 μL QUANTI-Blue reagent and incubated for 1 h at 37 °C before absorbance was measured at 655 nm. The percentage of neutralization was estimated with the equation below, where absorbance of TGF-β control ($A_{TGF\beta}$) was considered as 0% of neutralization (full effect of cytokine), and absorbance of media control without TGF-β (A_{media}) was considered as 100% of neutralization (no effect of cytokine).

$$\text{TGF}\beta \text{ neutralization } (\%) = \frac{A_{sample} - A_{TGF\beta}}{A_{media} - A_{TGF\beta}} \times 100\% \quad (1)$$

2.3. Full-Thickness Excision Wound Model

Female BALB/c mice were housed individually in the Center for Research and Assistance in Technology and Design in the State of Jalisco A. C. (CIATEJ), maintained on a 12-h light/dark cycle, and allowed ad libitum access to food and water. Experimental conditions adhered to the requirements defined by the Guidelines of the Institutional Animal Care and Use Committee (CICUAL). All assays fulfilled the Mexican regulations NOM-062-ZOO-1999. The animal facility has SENASICA certification AUT-B-B1115-025.

Mice (23–26 g weight and 12 weeks old) were anesthetized with isoflurane before dorsal surfaces were shaved and bilateral surgical wounds performed under sterile conditions with aseptic and antiseptic techniques. Two circular full-thickness skin wounds (2 mm diameter) were created with a disposable biopsy punch on each side of the mouse dorsum to include the panniculus carnosus layer (Integra Miltex, York, PA, USA). The right dorsal wound of each mouse was treated with the hydrogel (i.e., CAPH, CAPH-1D11-10, CAPH-1D11-50, or CAPH-1D11-100) while the left side of the same animal was left untreated as the control.

Mice were randomly assigned to four groups (5 mice per group): Group 1 represented the hydrogel control without anti-TGFβ antibody 1D11.16.8 (CAPH); Group 2 received CAPH with 10 μg anti-TGFβ (CAPH-1D11-10); Group 3 received CAPH with 50 μg anti-TGFβ (CAPH-1D11-50); and Group 4 received CAPH with 100 μg anti-TGFβ (CAPH-1D11-100).

2.3.1. Macroscopic Evaluation of Wound Healing

Body weight and general health were monitored throughout the experiment for 10 days. Wound healing was carefully monitored with digital photographs taken at days 0, 2, 4, 7, and 10, and by measuring wound diameter at each time-point. A semi-quantitative four-point score—0 (none), 1 (scant), 2 (moderate), and 3 (abundant)—was used for evaluating macroscopic physiological healing parameters, including: exudation, re-epithelialization, papule, erythema, inflammation, granulation tissue, hemorrhage, and necrosis [26]. Re-epithelialization was scored as: (0) absent, bright-red wound; (1) moderate presence of epithelialization surrounding granulation tissue, pink wound; (2) the presence of epithelialization exceeds that of granulation tissue, pale wound; and (3) fully healed wound [27–29]. Inflammation of the wound was determined by the presence of tissue bulging accompanied by erythema, and scored as (0) absent, (1) scant presence in the wound surroundings, (2) moderate presence outside the edges of the wound, and (3) completely surrounding the wound [30]. Each parameter was presented as a global score calculated by averaging the scores of all evaluated time-points.

2.3.2. Histological Analysis

All mice were euthanized on day 10 with an intraperitoneal injection of sodium pentobarbital (120 mg/kg). The wounded area and 5 mm margin of surrounding intact skin were collected for RT-PCR and histological evaluation with hematoxylin and eosin (H&E) and Masson's trichrome (MT) stains. Samples were fixed in 10% formalin for 24 h before being embedded in a paraffin wax block and cross-sectioned (6–8 µm). H&E staining was observed under 100× magnification to evaluate re-epithelialization and inflammation (i.e., granulated tissue), while collagen deposits and fibrosis were visualized by MT staining (also under 100× magnification). Optical collagen density was quantified from MT-stained sections with FIJI/ImageJ (NIH, v 2.0.0), images were converted to RGB, and the blue channel was used to analyze the collagen fibers [31].

2.4. RNA Isolation, Reverse Transcription, and Real-Time PCR Analysis

RNA was isolated from skin samples using a tissue homogenizer and RiboZol reagent (Amresco LLC, Solon, OH, USA) according to manufacturer's instructions. cDNA was synthesized from 500 ng RNA using the RevertAid First Strand cDNA Synthesis Kit (Thermo Fisher Scientific, Inc., Waltham, MA, USA). Real-time PCR was performed on the resultant cDNA using EvaGreen 5X qPCR mix (qARTA Bio Inc., Carson, CA, USA) and 10 pmol/µL forward and reverse primers in a LightCycler 96 (Roche Diagnostics, Mannheim, Germany). The amplification conditions consisted of 1 cycle of initial denaturation at 95 °C for 15 min followed by 40 cycles of denaturation at 95 °C for 15 s, annealing at 56 °C for 20 s, and extension at 72 °C for 20 s. The primers used to amplify Transforming growth factor beta 1 (*Tgfb1*), alpha-smooth muscle actin (*Acta2*), and hypoxanthine phosphoribosyltransferase (*Hprt*) are shown in Table 1. *Hprt* was used as an internal control to normalize gene expression data. The relative quantities of mRNA expression were determined using the $2^{-\Delta\Delta Ct}$ method.

Table 1. Primer sequences for real-time PCR analysis.

Gene	Name	Primer (5′-3′)
Tgfb1	Transforming growth factor beta	Forward: CACTCCCGTGGCTTCTAGTG Reverse: GGACTGGCGAGCCTTAGTTT
Acta2	Alpha-smooth muscle actin	Forward: TCAGCGCCTCCAGTTCCT Reverse: AAAAAAAACCACGAGTAACAAATCAA
Hprt	Hypoxanthine phosphoribosyltransferase	Forward: GTAATGATCAGTCAACGGGGGAC Reverse: CCAGCAAGCTTGCAACCTTAACCA

2.5. Statistical Analysis

All statistical analyses were performed using Prism 8.0 (GraphPad Software, Inc., San Diego, CA, USA). Data were expressed as mean ± Standard Error of the Mean (SEM). For HEK-Blue reporter cell assays, differences between multiple groups were evaluated by a one-way analysis of variance (ANOVA) followed by a Tukey's test. Wound closure in response to anti-TGF-β loaded CAPH (i.e., CAPH-1D11) was compared with CAPH by a two-way ANOVA, followed by a Dunnett's test. The differences observed between treated and untreated wounds following macroscopic evaluation of epithelialization and inflammation, collagen density, and real-time PCR analysis were determined by t-test. In all statistical comparisons, differences were deemed significant when p values < 0.05.

3. Results and Discussion

3.1. HEK-Blue TGF-β SEAP Reporter Cells Assay

Previous studies reported increased stability in CAPH compared to Ca-alginate hydrogels [20], along with the capacity of CAPH to store antibodies due to simple electrostatic interactions facilitated by PEGMA that can form acid–ether hydrogen bonds and create hydrophobic associations [32,33]. In the study reported here, neutralization of TGF-β by 1D11 antibodies released from hydrogels was evaluated in vitro and is presented in Figure 1. The findings show that CAPH-1D11 retained viability of 1D11 and enabled antibody release after being suspended in media for two hours. This period of time was determined previously using a control antibody, where a plateau of liberation was reached at two hours (data not shown). The results show that 1D11 was stable in solution, following lyophilization, and after being released from the hydrogel. However, the TGF-β neutralizing activity of 1D11 antibodies released from CAPH-1D11-1µg was approximately 70% and significantly lower than the lyophilized and solution 1D11 controls. It is possible that this reduced activity may be due to limited release of 1D11 from CAPH-1D11 after only two hours in media. Interestingly, CAPH without antibodies showed slight neutralizing activity of approximately 30%. Previous studies have reported that alginate can prevent TGF-β signaling by downregulating Smad2 phosphorylation and TGF-β expression [34–36]. However, calcium release could be another factor contributing to the observed neutralizing activity. Organista-Juárez et al. [37] showed in vitro using hepatic C9 cells and transfected HEK293 cells that exogenous administration of calcium decreases TGF-β dependent transcriptional activity through the calcium-sensing receptor (CaSR), interfering with Smad2 phosphorylation and inducing proteasomal degradation of Smad2.

3.2. Wound Contraction

To determine if CAPH-1D11 could retain the viability of 1D11 and enable antibody release in situ, CAPH and CAPH-1D11 were assessed in a mouse model of dorsal bilateral excisional wound healing [38–40] to observe the impact of TGF-β neutralization on wound healing parameters. Wound closure was evaluated for ten days to ensure a comprehensive assessment of the impact of TGF-β neutralization on wound healing. During this period, it was assumed wound healing would progress through the fibroblast and keratinocyte proliferation phase and enter the first stage of matrix remodeling (on day seven), characterized by ECM formation and collagen deposition [11,41]. Figure 2 illustrates the progress of wound closure over the course of the ten-day study. The findings show that the application of CAPH-1D11-10 resulted in the lowest wound diameter at day ten, while delays in wound closure were observed in response to CAPH-1D11-100. Overall, wound sizes did not vary significantly between groups at any experimental time point (Figure 2b). Expansion of the wound was observed in the first day and is often described in the early stages of excisional wound healing models as a result of tissue loosening [31,42].

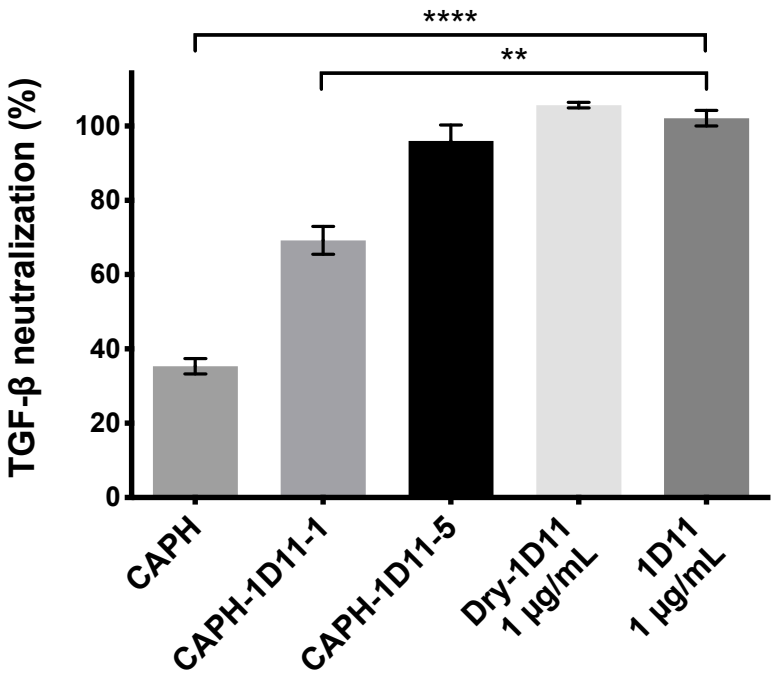

Figure 1. In vitro assessment of transforming growth factor-beta (TGF-β) neutralization by pan-specific anti-TGF-β mouse monoclonal antibody 1D11.16.8 released from loaded Ca-alginate-poly(ethylene glycol) methyl ether methacrylate (PEGMA) hydrogels. HEK-Blue TGF-β cells were used to evaluate the capacity of Ca-alginate-PEGMA hydrogels (CAPH) loaded with 1 and 5 µg 1D11.16.8 (CAPH-1D1-1 and CAPH-1D11-5, respectively) to release stable antibodies and neutralize 20 pM rhTGF-β1. Dry-1D11 is a reconstituted antibody that was lyophilized and 1D11 is a soluble antibody without any drying. Each bar represents the mean ± SEM of 3 independent assays conducted in triplicate. Significance denoted by ** $p < 0.01$ and **** $p < 0.0001$.

Macroscopic assessment of the wounds showed no papule, exudation, hemorrhage, or necrosis, and granulation tissue was similar across all groups (data not shown). Macroscopic epithelialization and inflammation were also assessed (Figure 2c,d). TGF-β is a potent inhibitor of keratinocyte proliferation through the induction of G1 cell cycle arrest [43,44]. After treatment with CAPH-1D11-10 and CAPH-1D11-50, epithelialization scores increased, coinciding with a reversal in the proliferative arrest of keratinocytes and promoting epidermal recovery. These findings agree with a study by Mandapalli et al. [45], where treatment with a TGF-β siRNA or crocodile oil accelerated re-epithelialization and reduced TGF-β1 and Smad3 protein and mRNA levels [46]. However, in the study presented here, epithelialization scores of wounds treated with CAPH-1D11-100 were similar to control wounds. This effect was possibly due to the negative impact of excessive TGF-β neutralization in the wound environment, resulting in non-healing chronic wounds where the ECM is not organized for efficient keratinization [47,48]. This assumption may also explain the delay in wound closure observed following CAPH-1D11-100 treatment.

In the inflammation phase of wound healing, TGF-β has dual roles as a pro-inflammatory stimulus early in the phase and as a potent anti-inflammatory chemoattractant of immune cells, such as neutrophils or monocytes, towards the end of this phase [49]. In Figure 2d, reduced inflammation scores in wounds following treatment with CAPH-1D11 may be explained by a decrease in immune cell infiltration through neutralization of the chemoattractant activity of TGF-β.

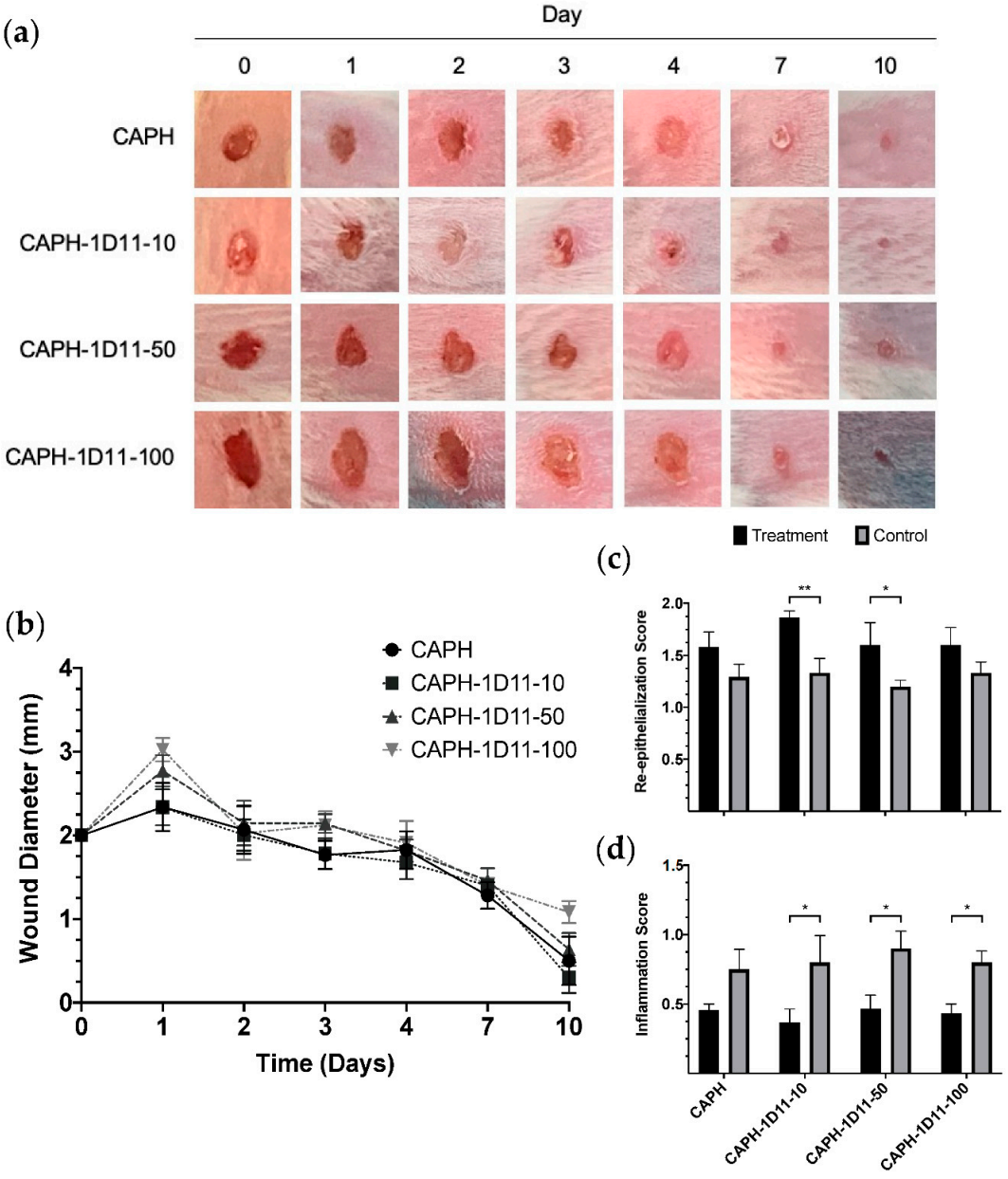

Figure 2. Wound contraction and assessment in response to application of Ca-alginate-PEGMA hydrogels with and without pan-specific anti-TGF-β mouse monoclonal antibody 1D11.16.8, evaluated over ten days. (**a**) Representative photographs of excisional wounds before and after application of Ca-alginate-PEGMA hydrogel (CAPH) loaded without or with 10, 50, and 100 μg anti-TGF-β antibody (CAPH-1D11-10, CAPH-1D11-50, and CAPH-1D11-100, respectively), evaluated over 10 days. (**b**) Comparison of wound size over 10 days with initial wound size being 2 mm for all groups. Graphic presented as the mean of wound diameter size in mm ± SEM, n = 5/group. (**c**) Epithelization. (**d**) Inflammation score of mice treated with CAPH with and without anti-TGF-β antibody. A four-point score was used (with 0 score (none), 1 score (scant), 2 score (moderate), and 3 score (abundant)), and is presented as a mean ± SEM. n = 5/group. Significance is denoted as * $p < 0.05$ and ** $p < 0.01$.

3.3. Histological Observations

Histological analysis of wounds at day ten was performed by H&E and MT staining. In Figure 3, staining revealed the formation of thin epidermal layers in all samples. Furthermore, the application of CAPH-1D11-50 and CAPH-1D11-100 produced epidermal layers with irregular appearances compared to other groups. Previous studies have shown that alginate based wound dressings can promote fibroblast proliferation and collagen

deposition [35,50,51]. In this study, the application of CAPH combined with a low anti-TGF-β dose, such as CAPH-1D11-10, improved wound epithelialization (evidenced by a tighter epidermis), but without loss of collagen deposition similar to CAPH. However, experimental observations should be performed for longer than ten days to determine if CAPH-1D11-10 could prevent scarring.

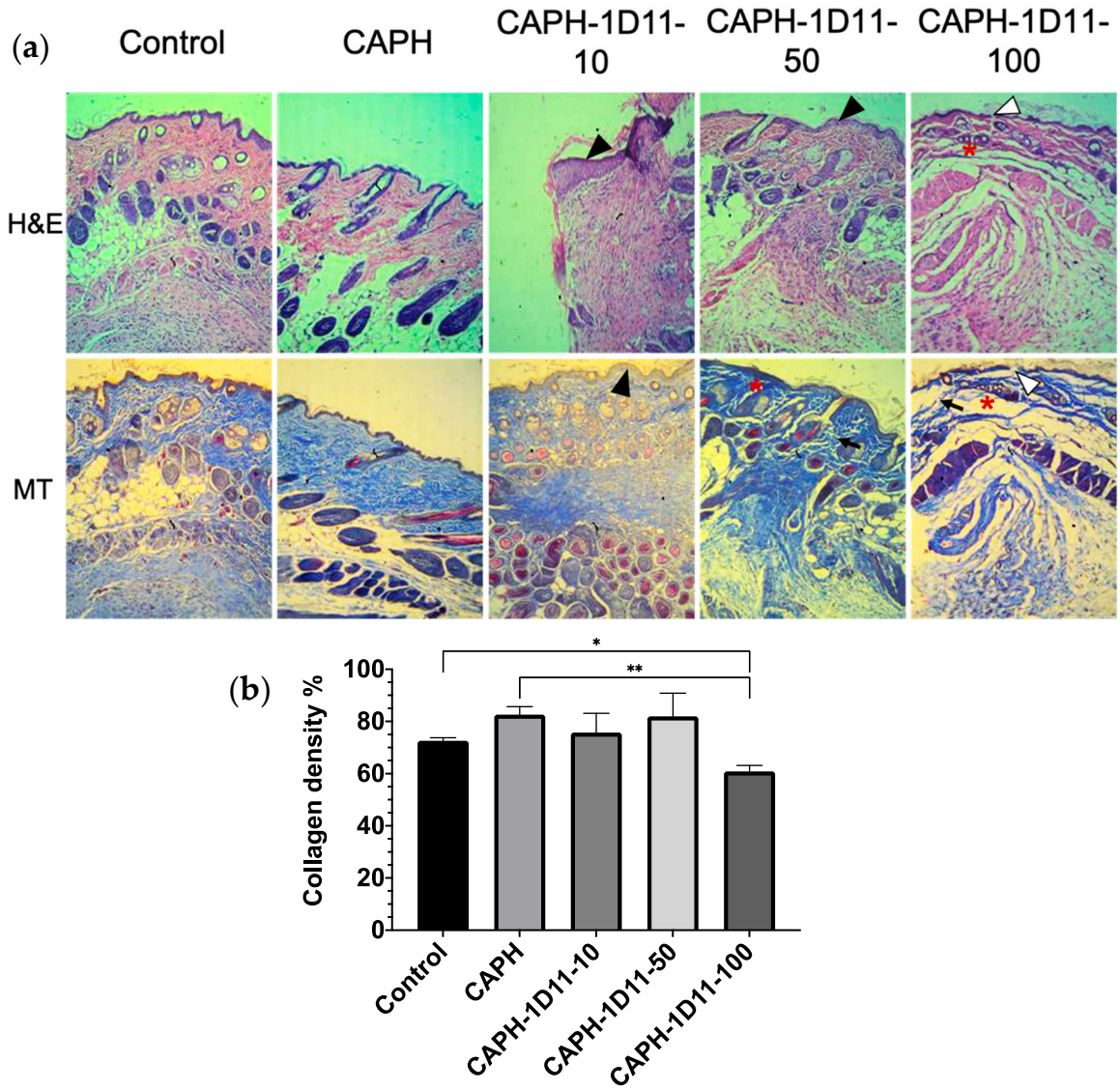

Figure 3. (**a**) Hematoxylin and eosin (H&E) and Masson's trichrome (MT) stained microscopic sections at day 10. Two excisional wounds were created on each dorsal side before Ca-alginate-PEGMA hydrogels (CAPH), or CAPH loaded with 10, 50, and 100 μg anti-TGF-β antibody (CAPH-1D11-10, CAPH-1D11-50, and CAPH-1D11-100, respectively) were applied to the right side. The wound on the left side received only standard disinfection treatment (Control). Micrographs of stained tissues were captured under 100X magnification. Application of CAPH-1D11-10 produced a tighter epidermis than other treatments (black arrowheads), while treatment with CAPH-1D11-50 produced irregular epidermal layers. Application of CAPH-1D11-100 produced epidermis and collagen fragmentation (white arrowheads and black arrows, respectively). Edematous zones (asterisks) are also indicated in CAPH-1D11-50 and CAPH-1D11-100 treated wounds. (**b**) Quantitative analysis of collagen density from blue channel of MT-stained sections. CAPH-1D11-100 treated wounds exhibit the lowest collagen density, presented as a mean ± SEM. n = 5/group. Significance is denoted as * $p < 0.05$ and ** $p < 0.01$.

In fibroblasts, the main promoter of collagen synthesis is TGF-β [52]. In Figure 3, MT staining of collagen fibers (in blue) revealed advanced collagen synthesis and remodeling with color intensity proportional to levels of deposited collagen [31,53]. Wounds treated

with CAPH-1D11-100 showed reduced collagen deposition (Figure 3b) and fragmented epidermal layers. In wound healing, TGF-β not only promotes collagen synthesis, but is also responsible for preventing collagen degradation by regulating the synthesis of several ECM proteases and inducing the secretion of specific protease inhibitors [54,55]. The appearance of fragmented collagen following the application of CAPH-1D11-50 and CAPH-1D11-100 could be attributed to enhanced collagen protease activity caused by TGF-β neutralization. However, the 1D11 antibody's affinity is biased towards TGF-β3 [56], the denominated "scarless" isoform of TGF-β. Lu et al. [24] described that a better response in wound healing is more associated with the temporary effect of TGF-β than with the specific neutralization of an isoform. They showed that neutralization of the three isoforms of TGF-β on the same day of wounding showed delayed wound healing without a reduction in hypertrophic markers. However, neutralization of TGF-β one-week post-wounding improved the hypertrophy. This effect correlates with the impaired wound healing showed in CAPH-1D11-100, which was administered the same day of wounding.

3.4. Reverse Transcription and Real-Time PCR Analysis

Reverse transcription and real-time PCR were used to measure mRNA levels of TGF-β and ACTA2 genes at day ten (Figure 4). TGF-β positively regulates its own expression in many cells [57], while TGF-β activation of fibroblasts to myofibroblast promotes expression of ACTA2 [58]. In this study, mRNA levels of *Tgfb1* and *Acta2* genes were significantly lower in lesions treated with CAPH-1D11-100 compared to control lesions. These findings indicate that CAPH-1D11-100 can release viable TGF-β neutralizing antibodies into wounds. Decreased TGF-β mRNA levels were also observed in response to CAPH, as previously described by Lee et al. (2009), but were not statistically different to the control.

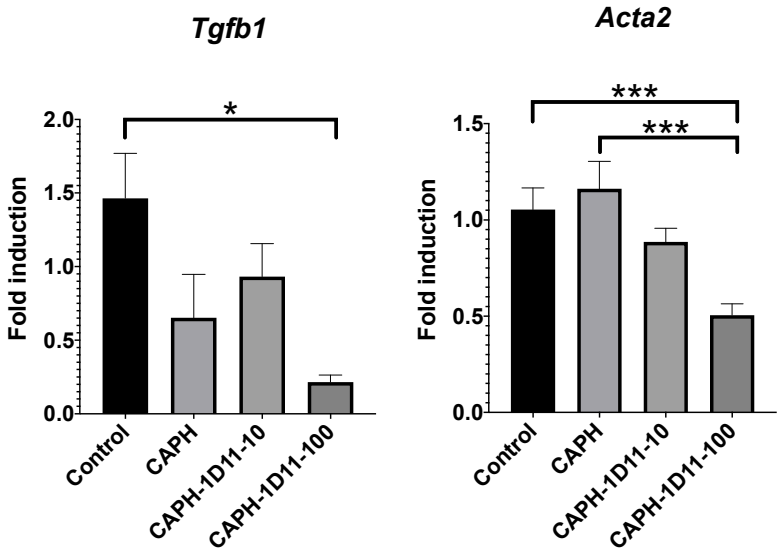

Figure 4. Reverse transcription and real-time PCR of transforming growth factor beta 1 (Tgfb1) and alpha-smooth muscle actin (Acta2) genes in skin lesions. mRNA levels of *Tgfb1* and *Acta2* genes were measured in skin lesions 10 days after treatment with Ca-alginate-PEGMA hydrogel (CAPH) or CAPH loaded with 10 or 100 µg 1D11.16.8 antibody (CAPH-1D11-10 and CAPH-1D11-100, respectively). Data were normalized to hypoxanthine phosphoribosyltransferase (HPRT) mRNA and presented as mean of fold induction (n = 5/group) ± SEM. Significance denoted as * $p < 0.05$ and *** $p < 0.001$.

ACTA2 is related to the capacity of myofibroblasts to promote wound contraction [59]. It is expected that the downregulation of the acta2 gene by CAPH-1D11-100 can lead to a decrease in wound closure. Although CAPH-1D11-100 exposed a trend in delayed wound closure, it was not significant because the expression of ACTA2 is beneficial but not

essential for wound contraction [60] since wound repair in mice is promoted primarily by the panniculus carnosus layer, which produces wound margins contracture [38,41].

4. Conclusions

In this study, a mouse model of dorsal bilateral excisional wound healing confirmed the capacity of Ca-alginate-PEGMA hydrogels to store, transport, and release TGF-β neutralizing antibodies at the site of a wound. Macroscopic assessment of the treated wounds revealed that wound sizes did not vary significantly between groups, and there was no evidence of papule, hemorrhage, or necrosis. Erythema surrounding each wound was also similar across all groups. Macroscopic epithelialization and inflammation were also assessed, revealing significantly reduced inflammation scores following application of all CAPH-1D11 treatments, while epithelialization significantly increased followed treatment with CAPH-1D11-10 and CAPH-1D11-50. The observations also supported a concomitant inhibition of fibrotic factors, such as collagen deposition and fibroblast to myofibroblast transition. Overall, these findings suggest that Ca-alginate-PEGMA hydrogels possess sufficient mechanical strength for the topical delivery of therapeutics. However, further studies are needed to explore the impact of Ca-alginate-PEGMA hydrogels loaded with anti-TGF-β antibodies on wound healing long-term.

Author Contributions: Conceptualization, A.B.C.-C. and A.F.L.-N.; methodology, A.F.L.-N., T.C.-V., P.H.L.-F., A.B.C.-C., N.E.D.-M., R.E. and E.P.-C.; formal analysis, J.G.-B., T.C.-V., R.E. and P.H.L.-F.; investigation, J.G.-B., T.C.-V., P.H.L.-F., A.B.C.-C., N.E.D.-M., R.E. and E.P.-C.; resources, A.F.L.-N., A.B.C.-C., N.E.D.-M., and E.P.-C.; writing—original draft preparation, J.G.-B.; writing—review and editing, T.C.-V., P.H.L.-F., A.B.C.-C. and A.F.L.-N.; supervision, A.F.L.-N.; project administration, A.F.L.-N.; funding acquisition, A.F.L.-N. All authors have read and agreed to the published version of the manuscript.

Funding: This research received no external funding.

Institutional Review Board Statement: The study was conduct according to the guidelines of the Care and Use of Laboratory Animals of the Center for Research and Assistance in Technology and Design of the State of Jalisco, A.C. (CIATEJ) and approved by the Institutional Animal Care and Use Committee (CICUAL) with number 2019-020A, in accordance with Mexican regulations "Technical specifications for production, care and use of laboratory animals" (NOM-062-ZOO-1999).

Acknowledgments: Jahaziel Gasperin-Bulbarela was supported by a CONACYT scholarship (No. 462358). Professional editing and proofreading were performed by Simone Osborne; Maria Echevarria for figure editing.

Conflicts of Interest: The authors declare no conflict of interest.

References

1. Kajdaniuk, D.; Marek, B.; Borgiel-Marek, H.; Kos-Kudła, B. Transforming growth factor beta1 (TGFbeta1) in physiology and pathology. *Endokrynol. Pol.* **2013**, *64*, 384–396. [CrossRef] [PubMed]
2. Pakyari, M.; Farrokhi, A.; Maharlooei, M.K.; Ghahary, A. Critical Role of Transforming Growth Factor Beta in Different Phases of Wound Healing. *Adv. Wound Care* **2013**, *2*, 215–224. [CrossRef] [PubMed]
3. Lichtman, M.K.; Otero-Vinas, M.; Falanga, V. Transforming growth factor beta (TGF-β) isoforms in wound healing and fibrosis. *Wound Repair Regen.* **2016**, *24*, 215–222. [CrossRef] [PubMed]
4. Gilbert, R.W.D.; Vickaryous, M.K.; Viloria-Petit, A.M. Signalling by transforming growth factor beta isoforms in wound healing and tissue regeneration. *J. Dev. Biol.* **2016**, *4*, 21. [CrossRef]
5. Le, M.; Naridze, R.; Morrison, J.; Biggs, L.C.; Rhea, L.; Schutte, B.C.; Kaartinen, V.; Dunnwald, M. Transforming Growth Factor Beta 3 Is Required for Excisional Wound Repair In Vivo. *PLoS ONE* **2012**, *7*, e48040. [CrossRef]
6. Occleston, N.L.; O'Kane, S.; Laverty, H.G.; Cooper, M.; Fairlamb, D.; Mason, T.; Bush, J.A.; Ferguson, M.W.J. Discovery and development of avotermin (recombinant human transforming growth factor beta 3): A new class of prophylactic therapeutic for the improvement of scarring. *Wound Repair Regen.* **2011**, *19*, s38–s48. [CrossRef]
7. Finnson, K.W.; Arany, P.R.; Philip, A. Transforming Growth Factor Beta Signaling in Cutaneous Wound Healing: Lessons Learned from Animal Studies. *Adv. Wound Care* **2013**, *2*, 225–237. [CrossRef]

8. Rice, L.M.; Padilla, C.M.; McLaughlin, S.R.; Mathes, A.; Ziemek, J.; Goummih, S.; Nakerakanti, S.; York, M.; Farina, G.; Whitfield, M.L.; et al. Fresolimumab treatment decreases biomarkers and improves clinical symptoms in systemic sclerosis patients. *J. Clin. Investig.* **2015**, *125*, 2795–2807. [CrossRef]
9. Lacouture, M.E.; Morris, J.C.; Lawrence, D.P.; Tan, A.R.; Olencki, T.E.; Shapiro, G.I.; Dezube, B.J.; Berzofsky, J.A.; Hsu, F.J.; Guitart, J. Cutaneous keratoacanthomas/squamous cell carcinomas associated with neutralization of transforming growth factor β by the monoclonal antibody fresolimumab (GC1008). *Cancer Immunol. Immunother.* **2015**, *64*, 437–446. [CrossRef]
10. Lee, K.Y.; Mooney, D.J. Alginate: Properties and biomedical applications. *Prog. Polym. Sci.* **2012**, *37*, 106–126. [CrossRef]
11. Sakai, S.; Sato, K.; Tabata, Y.; Kishi, K. Local release of pioglitazone (a peroxisome proliferator-activated receptor γ agonist) accelerates proliferation and remodeling phases of wound healing. *Wound Repair Regen.* **2016**, *24*, 57–64. [CrossRef]
12. D'Ayala, G.; Malinconico, M.; Laurienzo, P. Marine Derived Polysaccharides for Biomedical Applications: Chemical Modification Approaches. *Molecules* **2008**, *13*, 2069–2106. [CrossRef] [PubMed]
13. Naghshineh, N.; Tahvildari, K.; Nozari, M. Preparation of Chitosan, Sodium Alginate, Gelatin and Collagen Biodegradable Sponge Composites and their Application in Wound Healing and Curcumin Delivery. *J. Polym. Environ.* **2019**, *27*, 2819–2830. [CrossRef]
14. Ahmed, A.; Getti, G.; Boateng, J. Ciprofloxacin-loaded calcium alginate wafers prepared by freeze-drying technique for potential healing of chronic diabetic foot ulcers. *Drug Deliv. Transl. Res.* **2018**, *8*, 1751–1768. [CrossRef] [PubMed]
15. Stagnaro, P.; Schizzi, I.; Utzeri, R.; Marsano, E.; Castellano, M. Alginate-polymethacrylate hybrid hydrogels for potential osteochondral tissue regeneration. *Carbohydr. Polym.* **2018**, *185*, 56–62. [CrossRef]
16. Boateng, J.; Burgos-Amador, R.; Okeke, O.; Pawar, H. Composite alginate and gelatin based bio-polymeric wafers containing silver sulfadiazine for wound healing. *Int. J. Biol. Macromol.* **2015**, *79*, 63–71. [CrossRef]
17. Yeom, C.K.; Lee, K.H. Characterization of sodium alginate membrane crosslinked with glutaraldehyde in pervaporation separation. *J. Appl. Polym. Sci.* **1998**, *67*, 209–219. [CrossRef]
18. Afjoul, H.; Shamloo, A.; Kamali, A. Freeze-gelled alginate/gelatin scaffolds for wound healing applications: An in vitro, in vivo study. *Mater. Sci. Eng. C* **2020**, *113*, 110957. [CrossRef]
19. Santana, A.A.; Kieckbusch, T.G. Physical evaluation of biodegradable films of calcium alginate plasticized with polyols. *Braz. J. Chem. Eng.* **2013**, *30*, 835–845. [CrossRef]
20. Rubio-Elizalde, I.; Bernáldez-Sarabia, J.; Moreno-Ulloa, A.; Vilanova, C.; Juárez, P.; Licea-Navarro, A.; Castro-Ceseña, A.B. Scaffolds based on alginate-PEG methyl ether methacrylate-Moringa oleifera-Aloe vera for wound healing applications. *Carbohydr. Polym.* **2019**, *206*, 455–467. [CrossRef]
21. Dasch, J.R.; Pace, D.R.; Waegell, W.; Inenaga, D.; Ellingsworth, L. Monoclonal antibodies recognizing transforming growth factor-beta. Bioactivity neutralization and transforming growth factor beta 2 affinity purification. *J. Immunol.* **1989**, *142*, 1536–1541. [PubMed]
22. Shah, M.; Foreman, D.M.; Ferguson, M.W. Neutralising antibody to TGF-beta 1,2 reduces cutaneous scarring in adult rodents. *J. Cell Sci.* **1994**, *107 Pt 5*, 1137–1157.
23. Huang, J.S.; Wang, Y.-H.; Ling, T.-Y.; Chuang, S.-S.; Johnson, F.E.; Huang, S.S. Synthetic TGF-b antagonist accelerates wound healing and reduces scarring. *FASEB J.* **2002**, *16*, 1269–1270. [CrossRef]
24. Lu, L.; Saulis, A.S.; Liu, W.R.; Roy, N.K.; Chao, J.D.; Ledbetter, S.; Mustoe, T.A. The Temporal Effects of Anti-TGF-β1, 2, and 3 Monoclonal Antibody on Wound Healing and Hypertrophic Scar Formation. *J. Am. Coll. Surg.* **2005**, *201*, 391–397. [CrossRef]
25. Shah, M.; Foreman, D.M.; Ferguson, M.W. Neutralisation of TGF-beta 1 and TGF-beta 2 or exogenous addition of TGF-beta 3 to cutaneous rat wounds reduces scarring. *J. Cell Sci.* **1995**, *108*, 985–1002. [PubMed]
26. Tavares Pereira, D.D.S.; Lima-Ribeiro, M.H.M.; De Pontes-Filho, N.T.; Carneiro-Leão, A.M.D.A.; Correia, M.T.D.S. Development of animal model for studying deep second-degree thermal burns. *J. Biomed. Biotechnol.* **2012**, *2012*, 460841. [CrossRef] [PubMed]
27. Bloemen, M.C.T.; Boekema, B.K.H.L.; Vlig, M.; Van Zuijlen, P.P.M.; Middelkoop, E. Digital image analysis versus clinical assessment of wound epithelialization: A validation study. *Burns* **2012**, *38*, 501–505. [CrossRef] [PubMed]
28. Sardari, K.; Kakhki, E.G.; Mohri, M. Evaluation of wound contraction and epithelialization after subcutaneous administration of Theranekron® in cows. *Comp. Clin. Path.* **2007**, *16*, 197–200. [CrossRef]
29. Perez, D.; Bramkamp, M.; Exe, C.; von Ruden, C.; Ziegler, A. Modern wound care for the poor: A randomized clinical trial comparing the vacuum system with conventional saline-soaked gauze dressings. *Am. J. Surg.* **2010**, *199*, 14–20. [CrossRef]
30. Kadoyama, K.; Takenokuchi, M.; Matsuura, K.; Shichiri, H.; Watanabe, A.; Yamaguchi, H.; Takahashi, H.; Takano-Ohmuro, H.; Taniguchi, T. Therapeutic effects of shikonin on skin lesions in mouse models of allergic dermatitis and wound. *Tradit. Kampo Med.* **2019**, *6*, 62–70. [CrossRef]
31. Shin, D.Y.; Park, J.-U.; Choi, M.-H.; Kim, S.; Kim, H.-E.; Jeong, S.-H. Polydeoxyribonucleotide-delivering therapeutic hydrogel for diabetic wound healing. *Sci. Rep.* **2020**, *10*, 16811. [CrossRef] [PubMed]
32. Jones, J.A.; Novo, N.; Flagler, K.; Pagnucco, C.D.; Carew, S.; Cheong, C.; Kong, X.Z.; Burke, N.A.D.; Stöver, H.D.H. Thermoresponsive copolymers of methacrylic acid and poly(ethylene glycol) methyl ether methacrylate. *J. Polym. Sci. Part A Polym. Chem.* **2005**, *43*, 6095–6104. [CrossRef]
33. Hussain, H.; Mya, K.Y.; He, C. Self-assembly of brush-like poly[poly(ethylene glycol) methyl ether methacrylate] synthesized via aqueous atom transfer radical polymerization. *Langmuir* **2008**, *24*, 13279–13286. [CrossRef]

34. Feng, W.; Hu, Y.; An, N.; Feng, Z.; Liu, J.; Mou, J.; Hu, T.; Guan, H.; Zhang, D.; Mao, Y. Alginate Oligosaccharide Alleviates Monocrotaline-Induced Pulmonary Hypertension via Anti-Oxidant and Anti-Inflammation Pathways in Rats. *Int. Heart J.* **2020**, *61*, 160–168. [CrossRef] [PubMed]
35. Lee, W.R.; Park, J.H.; Kim, K.H.; Kim, S.J.; Park, D.H.; Chae, M.H.; Suh, S.H.; Jeong, S.W.; Park, K.K. The biological effects of topical alginate treatment in an animal model of skin wound healing. *Wound Repair Regen.* **2009**, *17*, 505–510. [CrossRef]
36. Xia, Z.; Ding, L.; Zheng, J.; Xu, Y.; Jin, W.; Sheng, X.; Wu, J. Alginate suppresses liver fibrosis through the inhibition of nuclear factor-κB signaling. *Drug Des. Dev. Ther.* **2020**, *14*, 1295–1305. [CrossRef]
37. Organista-Juárez, D.; Carretero-Ortega, J.; Vicente-Fermín, O.; Vázquez-Victorio, G.; Sosa-Garrocho, M.; Vázquez-Prado, J.; Macías-Silva, M.; Reyes-Cruz, G. Calcium-sensing receptor inhibits TGF-β-signaling by decreasing Smad2 phosphorylation. *IUBMB Life* **2013**, *65*, 1035–1042. [CrossRef]
38. Dunn, L.; Prosser, H.C.G.; Tan, J.T.M.; Vanags, L.Z.; Ng, M.K.C.; Bursill, C.A. Murine model of wound healing. *J. Vis. Exp.* **2013**, *2013*, 1–6. [CrossRef]
39. Grada, A.; Mervis, J.; Falanga, V. Research Techniques Made Simple: Animal Models of Wound Healing. *J. Investig. Dermatol.* **2018**, *138*, 2095–2105.e1. [CrossRef]
40. Rhea, L.; Dunnwald, M. Murine excisional wound healing model and histological morphometric wound analysis. *J. Vis. Exp.* **2020**, *2020*, 1–18. [CrossRef]
41. Zomer, H.D.; Trentin, A.G. Skin wound healing in humans and mice: Challenges in translational research. *J. Dermatol. Sci.* **2018**, *90*, 3–12. [CrossRef] [PubMed]
42. Ansurudeen, I.; Sunkari, V.G.; Grünler, J.; Peters, V.; Schmitt, C.P.; Catrina, S.B.; Brismar, K.; Forsberg, E.A. Carnosine enhances diabetic wound healing in the db/db mouse model of type 2 diabetes. *Amino Acids* **2012**, *43*, 127–134. [CrossRef] [PubMed]
43. Suzuki, D.; Pinto, F.; Senoo, M. Inhibition of TGF-β signaling promotes expansion of human epidermal keratinocytes in feeder cell co-culture. *Wound Repair Regen.* **2017**, *25*, 526–531. [CrossRef] [PubMed]
44. Liarte, S.; Bernabé-García, Á.; Nicolás, F.J. Role of TGF-β in Skin Chronic Wounds: A Keratinocyte Perspective. *Cells* **2020**, *9*, 306. [CrossRef] [PubMed]
45. Mandapalli, P.K.; Labala, S.; Jose, A.; Bhatnagar, S.; Janupally, R.; Sriram, D.; Venuganti, V.V.K. Layer-by-Layer Thin Films for Co-Delivery of TGF-β siRNA and Epidermal Growth Factor to Improve Excisional Wound Healing. *AAPS PharmSciTech* **2017**, *18*, 809–820. [CrossRef]
46. Li, H.L.; Chen, L.P.; Hu, Y.H.; Qin, Y.; Liang, G.; Xiong, Y.X.; Chen, Q.X. Crocodile oil enhances cutaneous burn wound healing and reduces scar formation in rats. *Acad. Emerg. Med.* **2012**, *19*, 265–273. [CrossRef]
47. Pastar, I.; Stojadinovic, O.; Krzyzanowska, A.; Barrientos, S.; Stuelten, C.; Zimmerman, K.; Blumenberg, M.; Brem, H.; Tomic-Canic, M. Attenuation of the transforming growth factor β-signaling pathway in chronic venous ulcers. *Mol. Med.* **2010**, *16*, 92–101. [CrossRef]
48. Kim, B.C.; Kim, H.T.; Park, S.H.; Cha, J.S.; Yufit, T.; Kim, S.J.; Falanga, V. Fibroblasts from chronic wounds show altered TGF-β-signaling and decreased TGF-β type II receptor expression. *J. Cell. Physiol.* **2003**, *195*, 331–336. [CrossRef]
49. Sanjabi, S.; Oh, S.A.; Li, M.O. Regulation of the immune response by TGF-β: From conception to autoimmunity and infection. *Cold Spring Harb. Perspect. Biol.* **2017**, *9*, a022236. [CrossRef]
50. Doyle, J.W.; Roth, T.P.; Smith, R.M.; Li, Y.Q.; Dunn, R.M. Effect of calcium alginate on cellular wound healing processes modeled in vitro. *J. Biomed. Mater. Res.* **1996**, *32*, 561–568. [CrossRef]
51. Caetano, G.F.; Frade, M.A.C.; Andrade, T.A.M.; Leite, M.N.; Bueno, C.Z.; Moraes, Â.M.; Ribeiro-Paes, J.T. Chitosan-alginate membranes accelerate wound healing. *J. Biomed. Mater. Res. Part B Appl. Biomater.* **2015**, *103*, 1013–1022. [CrossRef] [PubMed]
52. Varga, J.; Rosenbloom, J.; Jimenez, S.A. Transforming growth factor β (TGFβ) causes a persistent increase in steady-state amounts of type I and type III collagen and fibronectin mRNAs in normal human dermal fibroblasts. *Biochem. J.* **1987**, *247*, 597–604. [CrossRef] [PubMed]
53. Jiang, D.; Christ, S.; Correa-Gallegos, D.; Ramesh, P.; Kalgudde Gopal, S.; Wannemacher, J.; Mayr, C.H.; Lupperger, V.; Yu, Q.; Ye, H.; et al. Injury triggers fascia fibroblast collective cell migration to drive scar formation through N-cadherin. *Nat. Commun.* **2020**, *11*, 5653. [CrossRef] [PubMed]
54. Meng, X.; Nikolic-Paterson, D.J.; Lan, H.Y. TGF-β: The master regulator of fibrosis. *Nat. Rev. Nephrol.* **2016**, *12*, 325–338. [CrossRef] [PubMed]
55. Roberts, A.B.; McCune, B.K.; Sporn, M.B. TGF-β: Regulation of extracellular matrix. *Kidney Int.* **1992**, *41*, 557–559. [CrossRef] [PubMed]
56. Bedinger, D.; Lao, L.; Khan, S.; Lee, S.; Takeuchi, T.; Mirza, A.M. Development and characterization of human monoclonal antibodies that neutralize multiple TGF β isoforms. *MAbs* **2016**, *8*, 389–404. [CrossRef]
57. Van Obberghen-Schillin, E.; Roche, N.S.; Flanders, K.C.; Sporn, M.B.; Roberts, A.B. Transforming growth factor beta 1 positively regulates its own expression in normal and transformed cells. *J. Biol. Chem.* **1988**, *263*, 7741–7746. [CrossRef]
58. Desmouliere, A.; Geinoz, A.; Gabbiani, F.; Gabbiani, G. Transforming growth factor-β1 induces α-smooth muscle actin expression in granulation tissue myofibroblasts and in quiescent and growing cultured fibroblasts. *J. Cell Biol.* **1993**, *122*, 103–111. [CrossRef]
59. Goffin, J.M.; Pittet, P.; Csucs, G.; Lussi, J.W.; Meister, J.J.; Hinz, B. Focal adhesion size controls tension-dependent recruitment of α-smooth muscle actin to stress fibers. *J. Cell Biol.* **2006**, *172*, 259–268. [CrossRef]
60. Ibrahim, M.M.; Chen, L.; Bond, J.E.; Medina, M.A.; Ren, L.; Kokosis, G.; Selim, A.M.; Levinson, H. Myofibroblasts contribute to but are not necessary for wound contraction. *Lab. Investig.* **2015**, *95*, 1429–1438. [CrossRef]